

Periodic thin-film interference filters as one-dimensional photonic crystals

Dmitry N. Chigrin* and Clivia M. Sotomayor Torres

*Institute of Materials Science, Department of Electrical and Information Engineering
University of Wuppertal, D-42097 Wuppertal, Germany*

We review photonic band gap related properties of a simple periodic system of thin dielectric layers. Properties associated with forbidden and allowed bands of such one-dimensional photonic crystals are presented. A revision of forbidden bands properties leads to an *omnidirectional* Bragg mirror design. The anisotropy of allowed bands suggests the formation of *photon-focusing caustics* in one-dimensional photonic crystals.

I. INTRODUCTION

Artificial periodically microstructured dielectric materials have attracted widespread interest in recent years because of the possibility to alter the dispersion relation of photons [1–3]. Such periodic materials, *photonic crystals*, can exhibit energy gaps of zero density of states, *full photonic band gaps* (PBG). After the first suggestions of using photonic gaps to inhibit spontaneous emission [4–6] numerous attempts were made to realize three-dimensional (3D) structures that forbid visible light propagation in all directions (see e.g. [7]). Much less attention has been focused on the allowed bands of photonic crystals. The strong dispersion and spatial anisotropy of allowed bands lead to a number of new optical properties which are inconceivable in conventional crystals [8–11]. In contrast to a full PBG requiring a special topology of the 3D dielectric lattice, as well as considerably large refractive index contrast of constituents, strong dispersion and anisotropy of allowed bands are characteristic of any periodic structures even with a rather small index contrast.

The subject of this paper is the simplest type of photonic crystals, a periodic arrangement of dielectrics layers of alternating refractive indices, n_1 and n_2 , and thicknesses, d_1 and d_2 . Further, we use subscripts 1 and 2 for low and high index layers, respectively. Such kind of one-dimensional (1D) photonic crystals belong to the class of the well-known thin-film interference filters. Thin-film interference filters have proven to be of great importance in modern optoelectronic applications, ranging from Bragg mirrors for vertical cavity surface emitting lasers to narrow-band filters for dense wavelength division multiplexing systems (see e.g. [12–14]). However, it

has been shown recently that some passive devices based on interference filters can be improved if designed on the basis of photonic crystals [15–18].

In general, wave propagation in periodic media can be described in terms of Bloch waves. For clarity, Bloch waves are briefly discussed in Section II. Two examples associated with forbidden and allowed bands of a 1D photonic crystal are presented in Section III and Section IV, respectively. An example of an interference filter improvement is presented in Section III. Based on photonic band structure analysis we show how to make a Bragg mirror omnidirectional. In Section IV, a discussion of some photon-focusing caustics patterns in 1D photonic crystal is presented. Section V concludes the paper.

II. BLOCH WAVES

Optical properties of a periodic medium are described by its permittivity, which is a periodic function of a position in space. In the case of 1D photonic crystals a medium is periodic in one direction only, so the permittivity is: $\varepsilon(z) = \varepsilon(z + l\Lambda)$, where z is the direction of periodicity, $\Lambda = d_1 + d_2$ is the period, and l is an integer. According to the Bloch-Floquet theorem (see e.g. [14]), normal electromagnetic modes of such a periodic medium are

$$\mathbf{E} = \mathbf{E}_K(z) \exp(-iKz), \quad (1)$$

where $\mathbf{E}_K(z) = \mathbf{E}_K(z + l\Lambda)$ is a periodic function of period Λ . The subscript K is the Bloch wave number and indicates that the function $\mathbf{E}_K(z)$ depends on K . The field (1) can be expanded in Fourier series comprising an infinite set of partial waves, spatial harmonics. So, a traveling Bloch wave consists of a group of plane waves propagating together as a stable entity in a particular direction. To obtain a dispersion relation of an electromagnetic wave in a periodic medium, relating the frequency of a Bloch wave, ω , with the wave vector, \mathbf{k} , a Fourier expansion of (1) should be substituted into the Maxwell equations. This results in a dispersion relation in the form of an infinite system of linear equations. The system should be properly truncated to get a tractable numerical solution. An exact analytical solution is generally unavailable. Indeed, a 1D photonic crystal is a unique system for which an analytical form of the dispersion relation can be derived. Using the transfer matrix method one can obtain [14,19]:

*Author to whom correspondence should be addressed: e-mail: chigrin@uni-wuppertal.de

$$f(\omega, \mathbf{k}) = \cos(K\Lambda) - \left(\frac{1}{2}(A + D)\right) = 0. \quad (2)$$

A particular form of the functions $A(\omega, \mathbf{k}_\perp)$ and $D(\omega, \mathbf{k}_\perp)$ may be found elsewhere [14,19], here \mathbf{k}_\perp is the tangential component of the Bloch wave vector. The dispersion relation given by equation (2) contains all the information about photonic crystal eigenmodes, describing the properties of Bloch waves.

In general, the properties of Bloch waves in a periodic structure can differ drastically from those of a plane waves in an isotropic homogeneous medium. Well-known dispersion relation of a plane wave in an isotropic homogeneous nondispersive medium has a form

$$f(\omega, \mathbf{k}) = (\omega n/c)^2 - \mathbf{k}^2 = 0, \quad (3)$$

where n is the refractive index and c is the speed of light in vacuum. A 3D sketch of the dispersion relation (3), usually referred to as the light cone, is depicted in the figure 1(a). Only 2D slices of the wave vector space are presented. The main properties of the band structure are: (i) all polarization states are degenerate; (ii) there are not band gaps; and (iii) the direction of the energy flow, the direction of group velocity, \mathbf{v}_g , points parallel to the wave vector \mathbf{k} . The last property follows directly from the dispersion relation (3), because the group velocity is the gradient of the frequency ω in the wave vector space:

$$\mathbf{v}_g = \nabla_{\mathbf{k}} \omega(\mathbf{k}). \quad (4)$$

In a periodic 1D medium, even a small index perturbation yields a band structure that differs drastically from the light cone. In particular: (i) The polarization degeneracy is lifted. (ii) Photonic band gaps are developed. In the long wavelength limit, the band structure asymptotically follows the light cone of some homogeneous anisotropic uniaxial crystal, displaying so-called form birefringence [14,20]. For higher Bloch wave energies, new bands, which are separated by frequency and angular gaps appear in the band structure [Fig. 1(b)]. (iii) The energy flow does not follow the wave vector direction any more [Fig. 1(b)]. In a periodic media, the velocity of the energy flow integrated over a unit cell is still identical to the group velocity [21]. However, due to the strongly non-circular shape of constant-frequency contours in the wave vector space, the group velocity (4) is no longer parallel to the wave vector.

III. OMNIDIRECTIONAL REFLECTION

Probably one of the most famous application of thin-film interference filters is a Bragg mirror, which is a periodic alternation of different dielectric layers with low and high indices of refraction (Fig. 2). In general, mirrors

come in two basic varieties: a metallic mirror with a dissipative losses of few-percent, being in fact an omnidirectional reflector and a dielectric Bragg mirror. A dielectric Bragg mirror can be made nearly loss-less, but it is highly reflecting within only limited angular range. A structure, combining the properties of both mirror types, i.e., being omnidirectional and loss-less, is of strong interest as it is likely to find many applications in optoelectronics and all-optical systems.

Until recently, the possibility to design such a “perfect mirror” was mainly associated with 3D photonic crystals having a full PBG. Recently, several research groups worldwide have reported that a simple-to-fabricate Bragg mirror suffices to design a low-loss omnidirectional reflector [15–18]. This demonstration can lead to various high performance optoelectronic devices employed at any desirable wavelength. Efficient antenna substrates, energy saving filters, enclosures for microcavities [22] and waveguides [23] are a few potential applications.

The properties of Bloch waves inside a Bragg mirror are governed by the dispersion relation (2). Due to the planar geometry of the problem, the separation of the electromagnetic field into TE (transverse electric) and TM (transverse magnetic) polarization states is possible, where the electric or magnetic field vector is parallel to the layers interfaces, respectively. This splits the problem of light interaction with a Bragg mirror into two independent problems.

A projected band structure of an infinite periodic system of layers is depicted in the figure 3. This is a projection of a 3D band structure [Fig. 1(b)] onto the $\omega - k_x$ plane, where k_x is the tangential component of the wave vector \mathbf{k} , assuming that the plane of the incidence is $x-z$. The refractive indices, $n_1 = 1.4$ and $n_2 = 3.4$, are chosen close to ones of SiO_2 and Si in the near IR region. Thicknesses of the layers are equal ($d_1 = d_2$). The top panel is for TE polarization, and the bottom one for TM. An infinite periodic structure can support both propagating and evanescent Bloch waves. In figure 3, gray areas correspond to the propagating states, whereas white areas contain the evanescent states only and are referred to as photonic band gaps.

When the frequency and the wave vector of a wave, impinging externally at an angle, α_{inc} , from a homogeneous medium of refractive index, n , onto a thin-film stack, lies within the band gaps, an incident wave undergoes strong reflection. Pronounced high reflection bands (stopbands), depend strongly on frequency and angle of incidence. These can be easily understood from figure 3. Photonic band gaps (i) rapidly move to higher frequencies with increasing incident angle, denoted by the increase of the tangential component of the wave vector; (ii) the TM band gaps tends to zero when approaching the Brewster light-line, where $\omega = c|\mathbf{k}_\perp|/n_1 \sin \alpha_B$ (Fig. 3), $\alpha_B = \arctan n_2/n_1$ is the Brewster angle. The TM polarized wave propagates without any reflection from n_1

to n_2 layer, and from n_2 to n_1 layer, at the Brewster angle α_B . These properties of the band structure restrict the angular aperture of a polarization insensitive range of high reflectance.

In essence, omni-directional reflectance can be achieved due to the limitation of the number of modes that can be excited by externally incident waves inside the Bragg mirror. Light coming from the low-index ambient medium ($n < n_1, n_2$) is funneled into the internal cone narrowed by Snell's law (Fig. 2). Angles inside the crystal should be so small as to have band gaps open up to the grazing incident angles. In particular, *(i) sufficiently large index contrast of the layers with respect to the ambient medium ensures that light coming from the outside will never go below the Brewster's angle inside the crystal* (Fig. 2) and *(ii) sufficiently large refractive index contrast of the layers themselves can keep the band gaps open up to the grazing angles* [15–18].

A reduced region of k -space, where electromagnetic modes of the photonic crystals can be excited by externally incident wave, lies above the light-line (Fig. 3), which is a 2D projection of the light cone of an ambient medium. For example, in the case of the Si/SiO₂ structure in air the first two band gaps are open for all external angles of incidence (shaded areas in figure 3). No propagating mode are allowed in the stack for any propagating mode in the ambient medium for either polarizations. Thus, total omnidirectional reflection arises.

To demonstrate an omnidirectional Bragg mirror, transmission spectra of light impinging at normal and oblique (30°, 60°, 89°) angles of incidence onto the Si/SiO₂ structure are shown in figure 4. Here we assume for calculations that $d_2/(d_1 + d_2) \approx 0.324$ [18]. At normalized frequencies 0.25–0.32, a high reflectivity can be observed at all angles of incidence for both fundamental polarizations. Such a Bragg mirror can be treated as an omnidirectional high reflector with a relative bandwidth of about 25%. To obtain, e.g., an omnidirectional reflection centered at the radiation wavelength $\lambda = 1.5\mu m$, one needs a structure with a period of about $0.412\mu m$.

IV. PHOTON-FOCUSING CAUSTICS

The strongly non-spherical shape of constant-frequency surfaces of 1D photonic crystals [Fig. 1(b)] leads to an anisotropic energy flux. We will refer to this phenomenon as to *photon-focusing*, in analogy to *phonon-focusing*, which takes place for ballistic propagation of phonons in solids [24].

The anisotropy of periodic multilayer structures in the long-wavelength regime ($\lambda \gg \Lambda$) is a well known phenomenon [20], form birefringence. In the limit of long wavelengths, constant-frequency surfaces of electromagnetic modes in a photonic crystal are similar to the constant-frequency surfaces of a negative uniaxial crystal.

At shorter wavelengths, the anisotropy becomes stronger and constant-frequency surfaces become distorted, especially near the boundaries of the Brillouin zone [Fig. 1(b)].

The energy flow inside a photonic crystal is generally not along the direction of the wave vector. The energy propagates along the direction of the group velocity (4), i.e., along the outward normal to the constant-frequency surface. In fact, even a small perturbation of the refractive index suffices to distort drastically a constant-frequency surface from its original spherical shape. As a consequence, an isotropic distribution of wave vectors emanating from an isotropic photon source inside the crystal does not imply an isotropic distribution of energy flux.

To plot a constant-frequency surface of 1D photonic crystals, the dispersion relation (2) should be solved at a fixed frequency ω . In particular, one should vary the value of the tangential component of the wave vector \mathbf{k}_\perp and solve equation (2) for a Bloch wave number K , which is basically the k_z component of the Bloch wave vector. In figure 5 such a constant-frequency contour, which is an intersection of a constant-frequency surface by the $K - k_x$ plane, is depicted. To produce a 3D plot of a constant-frequency surface it is necessary to solve equation (2) for all wave vectors \mathbf{k}_\perp in the $k_x - k_y$ plane. However, 1D photonic crystals are invariant under any rotation around the normal to the layers boundaries. That is why, a constant-frequency surface of a 1D photonic crystal is simply a revolution surface of a 2D constant-frequency contour calculated in any plane perpendicular to the boundaries of the layers.

We plot a constant-frequency contours of a homogeneous isotropic (dashed curve) and a slightly modulated periodic multilayer (solid curve) media in figure 5. The refractive index of the homogeneous medium is $n = 3.4$ and a perturbation leads to a structure with indices $n_1 = 3.4$ and $n_2 = 3.41$. We further assume that layers thicknesses are equal ($d_1 = d_2$). Constant-frequency contours are presented for the normalized frequency $\omega = 0.146$, which is within a first band gap of the periodic medium. Near the Brillouin zone boundary the constant-frequency contour of photonic crystal is strongly non-circular. It consists of a concave and a convex regions with positive and negative Gaussian curvatures, respectively. The curvature of a photonic crystal constant-frequency contour is depicted in the inset to figure 5. In contrast to the constant curvature of a homogeneous medium (dashed line in the inset) the curvature of a photonic crystal displays a strong variation. There is an inflection point where the curvature vanishes (point A in Fig. 5).

It is known from phonon imaging experiments [24], that, in the geometrical optics approximation, a vanishing curvature of the constant-frequency surface leads to an infinite energy flux from a point source along the

corresponding group velocity direction. The geometrical optics approximation assumes that phonon (photon) wavelength is much smaller than the source and detector sizes, and certainly much smaller than the distance between the source and the detector. These sharp singularities in the energy flux are called *phonon-focusing caustics* [24].

Because the energy flux is inversely proportional to the curvature of the constant-frequency surfaces [24], the points with zero curvature (Fig. 5) will lead to *photon-focusing caustics* of electromagnetic energy flux inside the 1D photonic crystal. Due to the rotation invariance of a photonic crystal, the Gaussian curvature of the constant-frequency surface vanishes along the circle produced by the zero curvature point A (Fig. 5). If an isotropic non-coherent light source is placed inside a thick slab of 1D periodic medium, then sharply defined circular peaks in the intensity distribution should be detected outside the sample.

To substantiate this prediction we present a Monte Carlo simulation of an angular intensity distribution which is due to an isotropic point source inside the 1D photonic crystal. Our Monte Carlo intensity diagram construction process consists in generating a uniform random distribution of wave vectors \mathbf{k} and solving equations (2) and (4) to obtain group velocities of the electromagnetic modes belonging to each value of \mathbf{k} . Then the group velocity vectors are collected in all directions to form an angular plot of intensity.

The angular distribution depicted in figure 6 was generated with a large number (10^6) of initial wave vectors \mathbf{k} and a “source” situated inside the photonic crystal. The intensity was collected by a “detector” placed on the surface of the crystal along one of the layers boundary. An intense peak appears near the direction corresponding to the inflection point with zero curvature (point A in Fig. 5). This direction corresponds to 3.6° out of the normal to the crystal boundary. Figure 6 shows how the light intensity diminishes rapidly with increasing angular deviation from that direction. At observation angles around zero the vanishing intensity is due to the band gap of the photonic crystal.

V. CONCLUSION

In conclusion, we have presented a brief review of the properties of periodic thin-film interference filters, 1D photonic crystals. We have discussed an improvement of a Bragg mirror design. We have explained how to make a Bragg mirror omnidirectional. Finally we have predicted the formation of photon-focusing caustics in 1D photonic crystals. Being the simplest type of photonic crystals, thin-film interference filters, should be a good laboratory structure to study photonic band gap related

phenomena as well as a good candidates for improvement and design of optoelectronic devices. For example, problems of antenna on top of an omnidirectional mirror and microcavity with omnidirectional Bragg mirrors are interesting for further study.

ACKNOWLEDGMENTS

DNC wishes to dedicate this paper to his teacher and friend Andrei V. Lavrinenko, who introduced him to the world of electromagnetism of complex materials. This work was partially supported by the EU-IST project PHOBOS IST-1999-19009.

-
- [1] J. D. Joannopoulos, R. D. Meade, and J. N. Winn, *Photonic crystals: molding the flow of light* (Princeton University Press, Princeton NJ, 1995).
 - [2] *Confined electron and Photon: New physics and Applications*, E. Burstein and C. Weisbuch, eds., (Plenum Press, New York, 1995).
 - [3] *Photonic Band Gap Materials*, C. Soukoulis, ed., (Kluwer Academic, Dordrecht, 1996).
 - [4] V. Bykov, “Spontaneous emission in a periodic structure,” *Soviet Physics - JETP* **35**, 269–273 (1972).
 - [5] E. Yablonovitch, “Inhibited spontaneous emission in solid-state physics and electronics,” *Phys. Rev. Lett.* **58**, 2059 (1987).
 - [6] S. John, “Strong localization of photons in certain disordered dielectric superlattices,” *Phys. Rev. Lett.* **58**, 2486–2489 (1987).
 - [7] *Special issue on Electromagnetic crystal structures, design, synthesis, and applications*, A. Scherer, T. Doll, E. Yablonovitch, H. Everitt, and J. Higgins, eds., *J. Lightwave Tech.* **17**, 1928–2207 (1999).
 - [8] P. Russell, “Optics of Floquet-Block waves in dielectric gratings,” *Appl. Phys. B: Photophysics & Laser Chemistry* **B39**, 231–246 (1986).
 - [9] R. Zengerle, “Light propagation in singly and doubly periodic planar waveguides,” *J. Mod. Optics* **34**, 1589–1617 (1987).
 - [10] H. Kosaka, T. Kawashima, A. Tomita, M. Notomi, T. Tamamura, T. Sato, and S. Kawakami, “Superprism phenomena in photonic crystals,” *Phys. Rev. B* **58**, R10096–10099 (1998).
 - [11] H. Kosaka, T. Kawashima, A. Tomita, M. Notomi, T. Tamamura, T. Sato, and S. Kawakami, “Superprism phenomena in photonic crystals: toward microscale light-wave circuits,” *J. Lightwave Tech.* **17**, 2032–2038 (1999).
 - [12] H. Macleod, *Thin-Film Optical Filters* (Adam Hilger, Bristol, 1986).
 - [13] J. Rancourt, *Optical Thin Films: Users’ Handbook* (Macmillan Publishing Company, New York, 1987).
 - [14] P. Yeh, *Optical Waves in Layered Media* (John Wiley and Sons, New York, 1988).

- [15] Y. Fink, J. N. Winn, S. Fan, C. Chen, J. Michel, J. D. Joannopoulos, and E. L. Thomas, "A dielectric omnidirectional reflector," *Science* **282**, 1679 (1998).
- [16] D. N. Chigrin, A. V. Lavrinenko, D. A. Yarotsky, and S. V. Gaponenko, "Observation of total omnidirectional reflection from a one-dimensional dielectric lattice," *Appl. Phys. A: Materials Science and Processing* **68**, 25–28 (1999).
- [17] P. S. J. Russell, S. Tredwell, and P. J. Roberts, "Full photonic bandgaps and spontaneous emission control in 1d multilayer dielectric structures," *Opt. Commun.* **160**, 66–71 (1999).
- [18] D. N. Chigrin, A. V. Lavrinenko, D. A. Yarotsky, and S. V. Gaponenko, "All-dielectric one-dimensional periodic structures for total omnidirectional reflection and partial spontaneous emission control," *J. Lightwave Tech.* **17**, 2018–2024 (1999).
- [19] P. Russell, T. Birks, and F. Lloyd-Lucas, "Photonic Bloch waves and photonic band gaps," in *Confined electron and Photon: New physics and Applications*, E. Burstein and C. Weisbuch, eds., (Plenum Press, New York, 1995), pp. 585–633.
- [20] M. Born and E. Wolf, *Principles of Optics* (Pergamon, New York, 1980).
- [21] P. Yeh, "Electromagnetic propagation in birefringent layered media," *J. Opt. Soc. Am.* **69**, 742–756 (1979).
- [22] J. A. E. Wasey and W. L. Barnes, "Efficiency of spontaneous emission from planar microcavities," *J. Mod. Optics* **47**, 725–741 (2000).
- [23] Y. Fink, D. J. Ripin, S. Fan, C. Chen, J. D. Joannopoulos, and E. L. Thomas, "Guiding optical light in air using an all-dielectric structure," *J. Lightwave Tech.* **17**, 2039–2041 (1999).
- [24] J. Wolfe, *Imaging Phonons: Acoustic Wave Propagation in Solid* (Cambridge University Press, Cambridge, 1998).

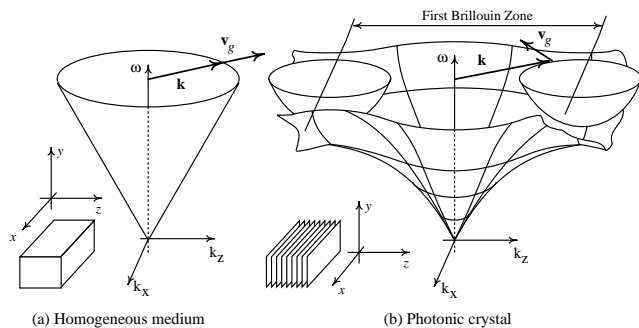


FIG. 1. A 3D representation of the photonic band structures of (a) an isotropic homogeneous nondispersive medium and (b) a 1D photonic crystal. Only 2D slices of the wave vector space are depicted. Insets show the orientation of the media. A photonic crystal band structure (b) is presented only for one basic polarization.

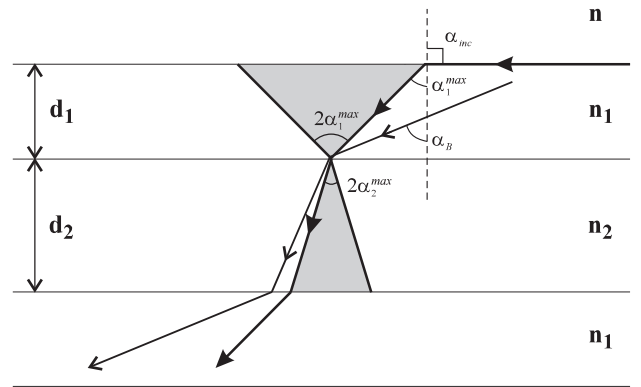


FIG. 2. Schematic representation of a dielectric multilayer structure. The light rays refracting and propagating through a stack are shown. The full domain of incident angles α_{inc} in the range from $-\pi/2$ to $\pi/2$ is mapped onto the internal cone of half-angle $\alpha_1^{max} = \arcsin n/n_1$ (light gray area).

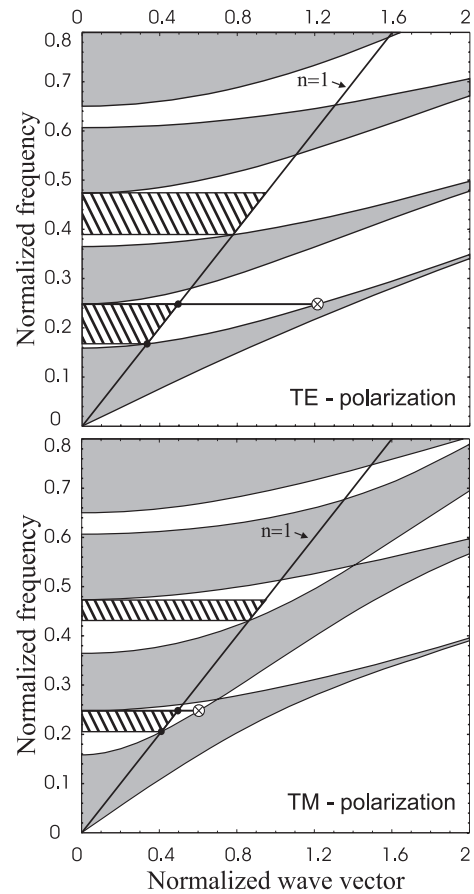


FIG. 3. Projected band structure of a typical 1D photonic crystal for TE (top panel) and TM (bottom panel) polarizations. The frequency and the tangential component of the wave vector are defined to be normalized as $\omega\Lambda/2\pi c$ and $|\mathbf{k}_\perp|\Lambda/\pi$, respectively. The gray areas correspond to the propagating states, whereas white areas contain the evanescent states only. The shaded areas correspond to omnidirectional reflection bands. The solid lines are the ambient-medium light-lines.

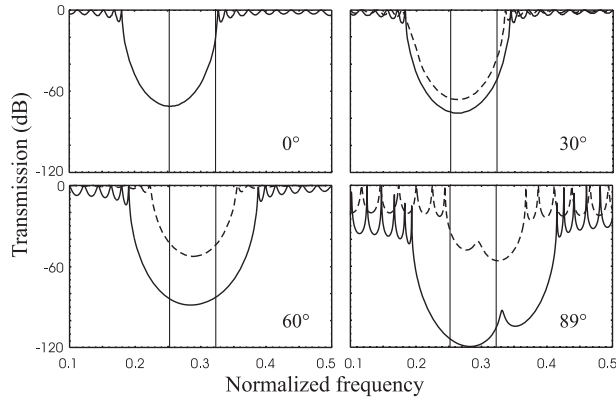


FIG. 4. Transmission spectra from a Si/SiO₂ structure with 10 periods at different incident angles, 0°, 30°, 60°, 89°. The solid (dashed) curves are for TE (TM) polarization. The vertical lines on each spectrum are the boundaries of a spectral region when omnidirectional reflection occurs.

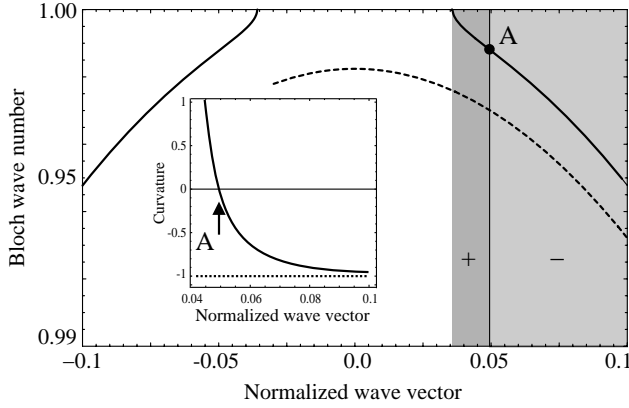


FIG. 5. $K - k_x$ intersection of dispersion surfaces of homogeneous isotropic (dashed curve) and slightly modulated periodic (solid curve) media. Normalized frequency is $\omega = 0.146$. Layers are of equal thickness. Inset shows a local curvature of the dispersion contour of photonic crystal. Arrow marks a wave vector for which the curvature is vanishing. Concave and convex region of constant-frequency contours are marked in different shades. Vertical and horizontal axes are not to scale.

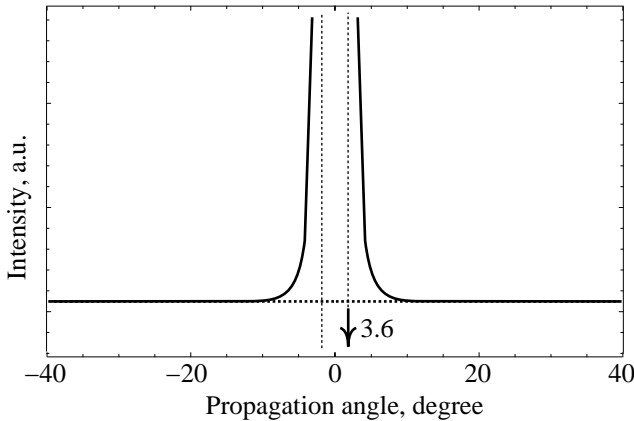


FIG. 6. Angular intensity distributions. Solid curve, photonic crystal, shows an intense peak in the direction corresponding to the inflection point. Dashed curve is an isotropic intensity distribution corresponding to a homogeneous medium.